THE JOURNAL OF BIOLOGICAL CHEMISTRY VOL. 285, NO. 40, pp. 30404–30410, October 1, 2010

A Single Amino Acid Tunes Ca^{2+} Inhibition of Brain Liver Intestine Na^+ Channel (BLINaC)

Received for publication, June 9, 2010, and in revised form, July 19, 2010 Published, JBC Papers in Press, July 23, 2010, DOI 10.1074/jbc.M110.153064

Dominik Wiemuth and Stefan Gründer[1]

From the Department of Physiology, RWTH Aachen University, D-52074 Aachen, Germany

Ion channels of the degenerin/epithelial Na^+ channel gene family are Na^+ channels that are blocked by the diuretic amiloride and are implicated in several human diseases. The brain liver intestine Na^+ channel (BLINaC) is an ion channel of the degenerin/epithelial Na^+ channel gene family with unknown function. In rodents, it is expressed mainly in brain, liver, and intestine, and to a lesser extent in kidney and lung. Expression of rat BLINaC (rBLINaC) in *Xenopus* oocytes leads to small unselective currents that are only weakly sensitive to amiloride. Here, we show that rBLINaC is inhibited by micromolar concentrations of extracellular Ca^{2+}. Removal of Ca^{2+} leads to robust currents and increases Na^+ selectivity of the ion pore. Strikingly, the species ortholog from mouse (mBLINaC) has an almost 250-fold lower Ca^{2+} affinity than rBLINaC, rendering mBLINaC constitutively active at physiological concentrations of extracellular Ca^{2+}. In addition, mBLINaC is more selective for Na^+ and has a 700-fold higher amiloride affinity than rBLINaC. We show that a single amino acid in the extracellular domain determines these profound species differences. Collectively, our results suggest that rBLINaC is opened by an unknown ligand whereas mBLINaC is a constitutively open epithelial Na^+ channel.

Ion channels of the degenerin/epithelial Na^+ channel (DEG/ENaC)[2] gene family share a Na^+-selective pore that is sensitive to block by the diuretic amiloride but are quite diverse concerning their functions and activating stimuli (1). They include constitutively active channels such as ENaC (2), mechanosensitive channels like the degenerins from *Caenorhabditis elegans* (3), and ligand-gated channels like H^+-gated ASICs (acid-sensing ion channels) (4) and like peptide-gated FaNaC (FMRFamide-gated Na^+ channel) (5) and HyNaCs (Hydra Na^+ channels) (6, 7).

Mammalian genomes typically contain nine genes coding for subunits of the DEG/ENaC channels: four genes code for ENaC subunits (α, β, γ, and δENaC; δENaC is absent in rodents; the ϵ subunit from *Xenopus laevis* (8) is probably the species ortholog of human δENaC) (9, 10), four code for ASICs (ASIC1–4) (1, 4), and one codes for the brain liver intestine Na^+ channel (BLINaC) (11). Whereas ENaC and ASICs have rather clearly defined functions and are implicated in several human diseases (12, 13), the function of BLINaC is completely unknown. BLINaC has initially been cloned from rat and mouse by homology to other DEG/ENaC channels (11). Its tissue distribution has been analyzed by reverse transcription-PCR and revealed predominant expression in rat brain, liver, and small intestine (hence its name). In mouse tissues, a similar distribution was found with additional expression in kidney and lung (11). The human ortholog, INaC (intestine Na^+ channel), is predominantly expressed in intestine (14). Although the localization of the BLINaC/INaC protein in those tissues is unknown, its predominant expression in nonneuronal tissues suggests that it might be involved in epithelial transport, like ENaC.

Functional expression of rat BLINaC and human INaC was investigated in *Xenopus* oocytes (11, 14). The proteins induced only a small constitutive current, which was unselective for Na^+ over K^+ and only partially blocked by amiloride ($IC_{50} > 1$ mM). Introduction of a constitutively activating mutation yielded currents that were rather selective for Na^+ over K^+ and blocked by amiloride with high affinity (IC_{50}, ~1 μM) (11, 14). These results suggested that BLINaC/INaC is a silent channel that is activated by a stimulus, which is still unknown. Because BLINaC is most closely related to ASICs and HyNaCs (6), this stimulus may be an extracellular ligand.

The gating mechanism of ASICs has been investigated in some detail (15) and might give hints to the gating mechanism of BLINaC. Extracellular H^+ and Ca^{2+} compete for binding sites on ASICs (16) and complete removal of extracellular Ca^{2+} opens ASICs (17, 18). One binding site for Ca^{2+} is in the outer mouth of ASICs, and a crucial component of this binding site is a conserved Asp residue (Asp^{432} in rat ASIC1a) (18).

Here, we revisit the functional properties of BLINaC. We found that, similar to ASICs, BLINaC is inhibited by extracellular Ca^{2+}, explaining the small currents of rat BLINaC (rBLINaC). Intriguingly, the apparent affinity for Ca^{2+} of mouse BLINaC (mBLINaC) is 250-fold lower than of rBLINaC, rendering mBLINaC constitutively active. Our results show that the activity of BLINaC is tightly regulated by $[Ca^{2+}]_e$ and uncovers profound species differences in constitutive channel activity.

EXPERIMENTAL PROCEDURES

Molecular Biology—Mouse BLINaC (GenBank accession no. NM_021370) was cloned by PCR from liver and rat BLINaC (GenBank accession no. NM_022227) from brain. Both cDNAs were subcloned into the expression vector pRSSP, which is optimized for functional expression in *Xenopus* oocytes, containing the 5′-untranslated region from *Xenopus* β-globin and a poly(A) tail (19). rBLINaC contained a

[1] To whom correspondence should be addressed: Dept. of Physiology, RWTH Aachen University, Pauwelsstrasse 30, D-52074 Aachen, Germany. Tel.: 49-241-80-88800; Fax: 49-241-80-82434; E-mail: sgruender@ukaachen.de.

[2] The abbreviations used are: DEG, degenerin; ENaC, epithelial Na^+ channel; ASIC, acid-sensing ion channel; BLINaC, brain liver intestine Na^+ channel; c, chicken; ECD, extracellular domain; HyNaC, Hydra Na^+ channel; INaC, intestine Na^+ channel; m, mouse; NMDG, *N*-methyl-D-glucamine; r, rat.

FLAG epitope in the extracellular domain (ECD) between amino acids Asp^{156} and Phe^{157}. Chimeras and single amino acid substitutions were generated by site-directed mutagenesis with KAPA HiFi polymerase (Peqlab) using standard protocols. PCR inserts were completely sequenced. Using the mMessage mMachine kit (Ambion, Austin, TX), capped cRNA was generated by SP6 RNA polymerase from linearized plasmids.

Electrophysiology—Oocytes were surgically removed under anesthesia (2.5 g/liter tricainemethanesulfonate for 20–30 min) from adult *X. laevis* females. Anesthetized frogs were killed after the final oocyte collection by decapitation. Animal care and experiments followed approved institutional guidelines at RWTH Aachen University.

Between 0.08 and 8 ng of cRNA was injected into stage V or VI oocytes of *X. laevis*. Oocytes were kept in low Na^+ OR-2 medium (5 mM NaCl, 77.5 mM *N*-methyl-D-glucamine, 2.5 mM KCl, 1.0 mM Na_2HPO_4, 5.0 mM HEPES, 1.0 mM $MgCl_2$, 1.0 $CaCl_2$, and 0.5 g/liter polyvinylpyrrolidone) at 19 °C and studied 24–48 h after injection. Whole cell currents were recorded with a TurboTec 03X amplifier (npi electronic, Tamm, Germany) using an automated, pump-driven solution exchange system together with the oocyte-testing carousel controlled by the interface OTC-20 (npi electronic) (20). With this system, 80% of the bath solution (10–90%) is exchanged within 300 ms (21). Data acquisition and solution exchange were managed using CellWorks version 5.1.1 (npi electronic). Data were filtered at 20 Hz and acquired at 1 kHz. Holding potential was −70 mV if not stated otherwise. All experiments were performed at room temperature (20–25 °C). The bath solution for two-electrode voltage clamp contained 140 mM NaCl, 1.8 mM $CaCl_2$, 1.0 mM $MgCl_2$, 10 mM HEPES. Low Ca^{2+} bath solutions contained 140 mM NaCl, 10 mM HEPES, 2 mM EDTA or H-EDTA and adequate amounts of $CaCl_2$ calculated with the program CaBuf (22). Solutions with Ca^{2+} concentrations <1.8 mM were supplemented with 0.1 mM flufenamic acid to block the large conductance induced in *Xenopus* oocytes by divalent-free extracellular solutions.

Data Analysis—Data were collected and pooled from at least two preparations of oocytes isolated on different days from different animals, if not stated otherwise. Data were analyzed with the software IgorPro (WaveMetrics, Lake Oswego, OR) and are presented as means ± S.E. Statistical significance was calculated using Student's unpaired *t* test.

The permeability ratio $P_H/P_{Na} = P'$ was calculated from the shift in reversal potential when proton concentration was raised from 100 nM (pH 7) to 100 μM (pH 4) using the following equation derived from the Goldman-Hodgkin-Katz equation,

$$\Delta E_{rev} = E_{rev,pH4} - E_{rev,pH7} = (RT/F)\ln(([Na^+]^1_0 + P'[H^+]^1_0)/([Na^+]^2_0 + P'[H^+]^2_0)) \quad \text{(Eq. 1)}$$

where R = ideal gas constant, T = absolute temperature, F = Faraday constant, $[Na^+]^1_0 = [Na^+]^2_0 = 10^{-3}$ M, $[H^+]^1_0 = 10^{-4}$ M, and $[H^+]^2_0 = 10^{-7}$ M. The effect of Ca^{2+}, Mg^{2+}, and *N*-methyl-D-glucamine (NMDG) in the extracellular solution was considered negligible. The intracellular concentration of K^+ was unknown but equal under both conditions and therefore did not affect the change in reversal potential ΔE_{rev}.

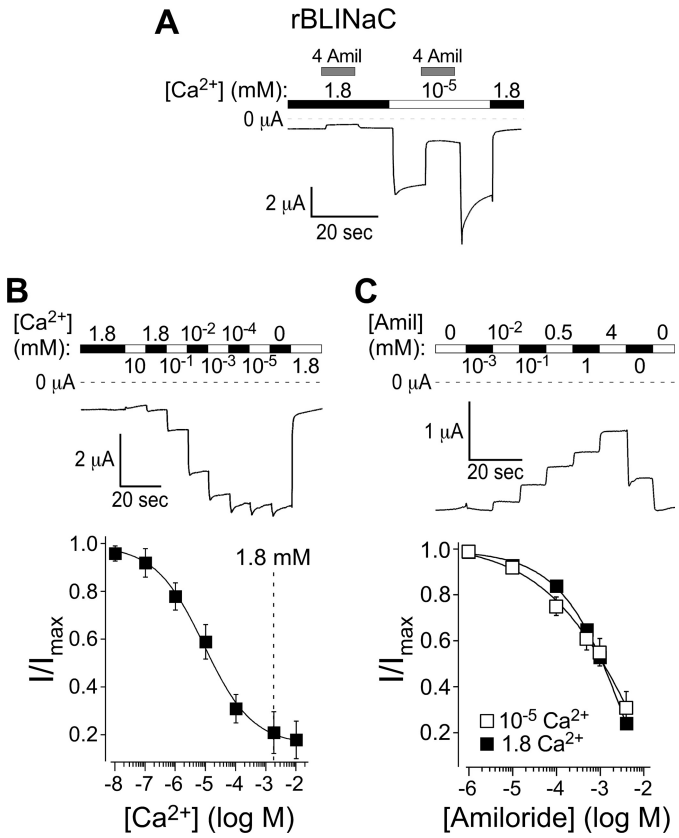

FIGURE 1. **Rat BLINaC is inhibited by physiological concentrations of extracellular Ca^{2+}.** *A*, representative current trace of oocytes expressing rBLINaC. Amiloride-sensitive (4 mM) current was recorded in 1.8 mM and 10 nM $[Ca^{2+}]_e$, respectively; holding potential was −70 mV. *B*, *upper*, representative current trace recorded in the presence of decreasing $[Ca^{2+}]_e$. *B*, *lower*, concentration-dependent inhibition of rat BLINaC by $[Ca^{2+}]_e$. Currents were normalized to the current in the presence of 10 nM $[Ca^{2+}]_e$; $n = 10$. The *dashed line* highlights a Ca^{2+} concentration of 1.8 mM. *Error bars*, S.E. *C*, *upper*, representative current trace recorded in the presence of increasing concentrations of amiloride (*Amil*); $[Ca^{2+}]_e$ was 1.8 mM. *C*, *lower*, concentration-dependent inhibition of rBLINaC by amiloride in physiological $[Ca^{2+}]_e$ (*filled squares*, $n = 10$) and low $[Ca^{2+}]_e$ (*open squares*, $n = 8$); currents were normalized to the current in the absence of amiloride.

RESULTS

Rat BLINaC Is Strongly Inhibited by Extracellular Ca^{2+}—Similar to previous findings (11), *Xenopus* oocytes expressing rBLINaC had only a slightly increased conductance compared with uninjected oocytes. The amplitudes of the small constitutive currents were in the range of 0.3–1.5 μA and only blocked by high concentrations (4 mM) of amiloride (Fig. 1*A*). Because the related ASICs are inhibited by extracellular Ca^{2+} (16–18), we wondered whether Ca^{2+} might also inhibit BLINaC. Reducing $[Ca^{2+}]$ in the bath solution to 10 nM indeed dramatically increased the amplitude of the amiloride-sensitive (4 mM) current to 11.6 ± 2.1 μA ($n = 11$; Fig. 1*A*). Determination of the current amplitude of rBLINaC-expressing oocytes with different concentrations of Ca^{2+} revealed an apparent IC_{50} for Ca^{2+} of 10 ± 1.5 μM ($n = 10$; Fig. 1*B*), revealing that rBLINaC is almost completely inhibited at physiological concentrations of extracellular Ca^{2+} (1.8 mM). With low concentrations of extracellular Ca^{2+}, however, BLINaC shows robust constitutive currents. Thus, $[Ca^{2+}]_e$ tightly controls rBLINaC activity.

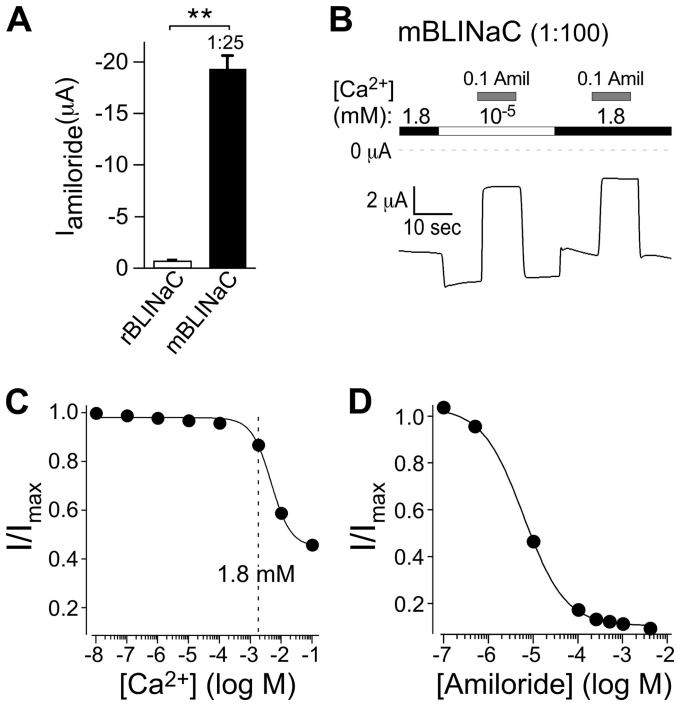

FIGURE 2. **Mouse BLINaC is constitutively open.** *A*, comparison of amiloride-sensitive current amplitudes of oocytes expressing rBLINaC (undiluted cRNA) or mBLINaC (25-fold diluted cRNA), $n = 8$, **, $p < 0.005$. *B*, representative current trace from an oocyte injected with 100-fold diluted mBLINaC. Amiloride-sensitive (100 μM) current was recorded in 1.8 mM and 10 nM $[Ca^{2+}]_e$, respectively. Holding potential was −70 mV. *C*, concentration-dependent inhibition of mBLINaC by $[Ca^{2+}]_e$. Currents were normalized to the current in the presence of 10 μM $[Ca^{2+}]_e$; $n = 16$. *D*, concentration-dependent inhibition of mBLINaC by amiloride; $n = 10$. Currents were normalized to the current in the absence of amiloride.

Amiloride is an open channel blocker that binds to the outer mouth of the DEG/ENaC pore (23). In ASICs, Ca^{2+} also binds to the outer mouth of the ion pore and competes there with amiloride, decreasing its apparent affinity (18). This finding suggested that the low amiloride sensitivity of rBLINaC (11) might be due to strong Ca^{2+} block at physiological concentrations of Ca^{2+}. To test this hypothesis, we determined the amiloride sensitivity also in the presence of 10 nM Ca^{2+}. However, block of rBLINaC was half-maximal at similar concentrations of amiloride, whether measured in physiological or low concentrations of Ca^{2+} ($IC_{50} = 6.4 \pm 1.7$ mM, $n = 8$, compared with 4.9 ± 1.3 mM, $n = 10$; $p = 0.5$; Fig. 1*C*), showing that the low amiloride sensitivity of rBLINaC is not due to Ca^{2+} block and suggesting that Ca^{2+} and amiloride do not compete for binding to the same site on the channel.

Mouse BLINaC Has a Dramatically Reduced Affinity for Extracellular Ca^{2+}—Next, we cloned the BLINaC ortholog from mouse and studied its electrophysiological characteristics. In strong contrast to rBLINaC, current amplitudes of oocytes expressing mBLINaC were >50 μA with physiological $[Ca^{2+}]_e$ (1.8 mM) when cRNA was injected undiluted (8 ng). Therefore, in the remainder of this study, for expression of mBLINaC, we injected oocytes with 25- or 100-fold diluted cRNA. When injected 25-fold diluted, the average current of mBLINaC-expressing oocytes was 19.3 ± 0.9 μA ($n = 8$), almost 25-fold higher ($p < 0.005$) than the current of rBLINaC-expressing oocytes (undiluted RNA) at 1.8 mM Ca^{2+} (Fig. 2*A*).

When we replaced the standard bath solution with a solution of low $[Ca^{2+}]_e$ (10 nM), the large constitutive mBLINaC current was further increased but only modestly (<1.2-fold, $n = 11$; Fig. 2*B*). Indeed, the apparent affinity for Ca^{2+} of mBLINaC was almost 250-fold lower ($IC_{50} = 2.3 \pm 0.2$ mM; $n = 10$; Fig. 2*C*) than for rBLINaC, showing that physiological concentrations of extracellular Ca^{2+} (1.8 mM) only modestly inhibit mBLINaC. Thus, in contrast to rBLINaC, mBLINaC is constitutively active at physiological concentrations of extracellular ions, revealing a dramatic species difference in apparent affinity for Ca^{2+} inhibition.

Application of high concentrations of amiloride (>100 μM; Fig. 2*B*) completely blocked mBLINaC, and block was half-maximal at ~700-fold lower concentrations of amiloride than for rBLINaC ($IC_{50} = 7.1 \pm 0.9$ μM, $n = 16$, $p < 0.005$; Fig. 2*D*). In summary, the comparative analysis of rat and mouse BLINaC revealed dramatic differences in the apparent affinity for Ca^{2+} and amiloride. Whereas rBLINaC is inhibited by physiological $[Ca^{2+}]_e$ and is active only in solutions with very low $[Ca^{2+}]_e$, mBLINaC is constitutively active at physiological $[Ca^{2+}]_e$.

A Single Amino Acid Determines the Different Apparent Affinities for Ca^{2+} and Amiloride of Rat and Mouse BLINaC—The functional differences between rat and mouse BLINaC were all the more surprising because their amino acid sequences are 97% identical. To identify the region responsible for the different Ca^{2+} affinities of rat and mouse BLINaC, we generated several chimeras and determined the amplitude of the amiloride-sensitive currents (4 mM) in 1.8 mM extracellular Ca^{2+} as a first indication for the apparent Ca^{2+} affinity of the chimeras.

First, we exchanged the cytosolic N- and C-terminal domains of rBLINaC by the corresponding domains of mBLINaC, either individually (chimeras "N-term" and "C-term") or together ("N/C-term"). The amiloride-sensitive current amplitude of these three chimeras was not increased compared with rBLINaC (Fig. 3*A*), suggesting that the cytosolic domains of rBLINaC do not determine the small current amplitude of these chimeras. In the next step, we exchanged the ECD of rBLINaC in two portions (chimeras "loop1" and "loop2"). Exchange of the first part of the ECD (loop1) did not increase the amplitude of the amiloride-sensitive current (Fig. 3*A*), whereas exchange of the second part of the ECD (loop2) strongly increased the amplitude of the amiloride-sensitive current to values comparable with mBLINaC (Fig. 3*A*). Moreover, although we did not systematically investigate amiloride sensitivity of these chimeras, the highly active chimera loop2 was almost completely blocked by 100 μM amiloride, showing that this chimera also had a lower IC_{50} for amiloride than rBLINaC.

To evaluate apparent Ca^{2+} affinity of the chimeras further, we measured current amplitude with 10 nM Ca^{2+} in the bath solution. This reduction in $[Ca^{2+}]_e$ strongly increased (3–8-fold; $n = 5$; $p < 0.005$) the current amplitude of all chimeras, except the highly active chimera loop2, for which the current amplitude was only modestly (1.1-fold, $n = 6$) increased (results not shown). This response to a reduction in $[Ca^{2+}]_e$ is in agreement with the idea that all chimeras, except loop2, had a high apparent Ca^{2+} affinity and were almost completely blocked by standard $[Ca^{2+}]_e$ (1.8 mM) and that the loop2 chimera had a

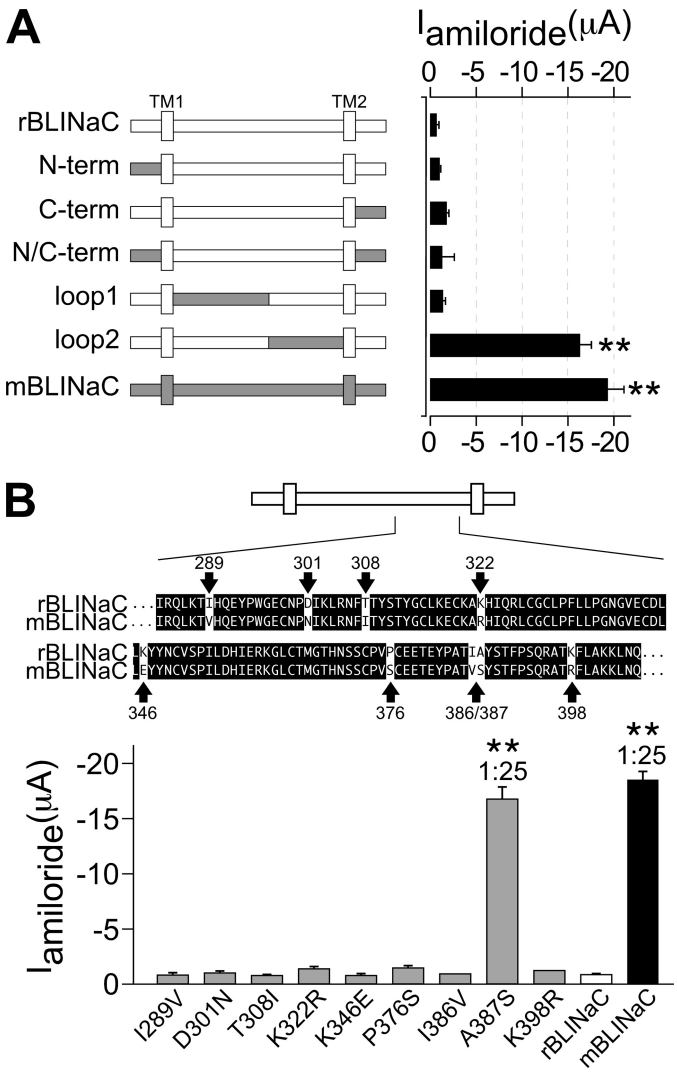

FIGURE 3. **A single amino acid is responsible for the species difference between rat and mouse BLINaC.** *A*, *left*, schematic drawings of rat and mouse BLINaC and chimeras. *A*, *right*, amiloride-sensitive current amplitudes of rat and mouse BLINaC and chimeras. 100 μM amiloride was used for mBLINaC and chimera loop2, 4 mM amiloride for all others. cRNA was injected undiluted except for mBLINaC and loop2, which were injected 25-fold diluted. Results represent data from 1 week, $n = 5$. **, $p < 0.005$. *Error bars*, S.E. *B*, *upper*, alignment of the amino acid sequences of the second part of the ECD of rat and mouse BLINaC. Amino acids different between rat and mouse are marked by *arrows*. *B*, *lower*, amiloride-sensitive current amplitudes of oocytes expressing rBLINaC carrying individual amino acid substitutions. 100 μM amiloride was used for mBLINaC and rBLINaC-A387S, 4 mM for all others. All cRNAs were injected undiluted except for mBLINaC and rBLINaC-A387S, which were injected 25-fold diluted. Results represent data from 1 week, $n = 8$. **, $p < 0.005$.

lower apparent Ca^{2+} affinity, leading to a modest block of this chimera by standard $[Ca^{2+}]_e$. Together, these results strongly suggest that the second portion of the ECD determines apparent Ca^{2+} affinity of BLINaC.

Within the second portion of the ECD, mouse and rat BLINaC differ in nine amino acids. We individually substituted these nine amino acids in rBLINaC by those of mBLINaC and determined the amplitude of the amiloride-sensitive (4 mM) currents in 1.8 mM extracellular Ca^{2+}. Eight of the nine substitutions did not significantly increase the current amplitude compared with wt rBLINaC (Fig. 3*B*). One substitution, however, A387S, dramatically increased the current amplitude of

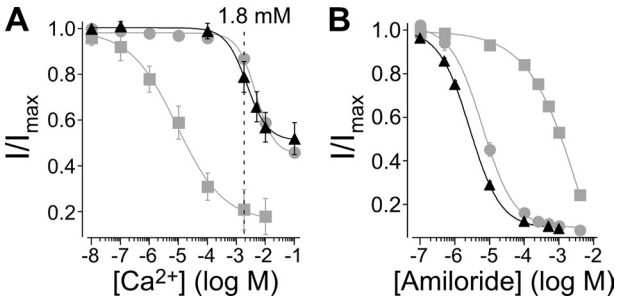

FIGURE 4. **Amino acid 387 determines Ca^{2+} affinity and amiloride affinity of BLINaC.** *A*, concentration-dependent inhibition of rBLINaC-A387S by $[Ca^{2+}]_e$ (*black triangles*). Currents were normalized to the current in the presence of 10 μM $Ca^{2+}{}_e$, $n = 11$. Dose-response curves of rBLINaC (*gray squares*) and mBLINaC (*gray circles*) from Figs. 1*B* and 2*C*, respectively, are shown for comparison. *B*, concentration-dependent inhibition of rBLINaC-A387S by amiloride (*black triangles*). Currents were normalized to the current in the absence of amiloride, $n = 14$. Dose-response curves of rBLINaC (*gray squares*) and mBLINaC (*gray circles*) from Figs. 1*C* and 2*D*, respectively, are shown for comparison.

rBLINaC to levels not significantly different from mBLINaC (Fig. 3*B*). In fact, like mBLINaC, rBLINaC-A387S had to be injected in a 1:25 dilution to get current amplitudes <50 μA. This robust current in the presence of physiological $[Ca^{2+}]_e$ suggested that the apparent Ca^{2+} affinity of rBLINaC was strongly decreased by the A387S substitution. This was indeed the case: the apparent Ca^{2+} affinity of rBLINaC-A387S was 500-fold lower (IC_{50}: 5.0 $\pm$ 0.3 mM, $n = 11$; Fig. 4*A*) than that of wild-type (WT) rBLINaC and in a millimolar range similar to that of mBLINaC.

Similar to chimera loop2, the rBLINaC-A387S substitution was strongly blocked by 100 μM amiloride (Fig. 3*B*), and amiloride sensitivity of rBLINaC-A387S was dramatically increased (IC_{50}: 2.9 $\pm$ 0.3 μM, $n = 14$; Fig. 4*B*) compared with WT rBLINaC and similar to mBLINaC. Thus, the single Ala to Ser substitution at position 387 explains both the different apparent Ca^{2+} and amiloride affinities of rat and mouse BLINaC.

Rat and Mouse BLINaC Have Different Ion Selectivities, Which Are Determined by Amino Acid 387—Besides small current amplitude and low apparent amiloride affinity, WT rBLINaC is characterized by unselectivity for monovalent cations (11), a feature that is rather uncommon for DEG/ENaC channels (1). To investigate ion selectivity of BLINaC, we first determined reversal potentials of rBLINaC, mBLINaC, and rBLINaC-A387S in physiological $[Ca^{2+}]_e$. The reversal potential of rBLINaC was -9.6 ± 2.0 mV ($n = 8$; Fig. 5*A*), similar to previous results (11), whereas it was significantly more positive for mBLINaC (14.6 $\pm$ 1.8 mV, $n = 10$; $p \ll 0.001$; Fig. 5*A*), indicating an increased selectivity for Na^+. For rBLINaC-A387S, the reversal potential was similar to mBLINaC (15.4 $\pm$ 1.6 mV, $n = 8$; Fig. 5*A*), indicating that this amino acid substitution also converted ion selectivity. Oocytes expressing mBLINaC and rBLINaC-A387S had a more positive membrane potential than oocytes expressing rBLINaC (data not shown), suggesting higher intracellular Na^+ concentrations in these oocytes due to the much stronger activity of mBLINaC and rBLINaC-A387S. Considering that higher intracellular Na^+ concentrations will reduce the Na^+ equilibrium potential, a reversal potential of ~15 mV indicates that mBLINaC is a Na^+-selective ion channel.

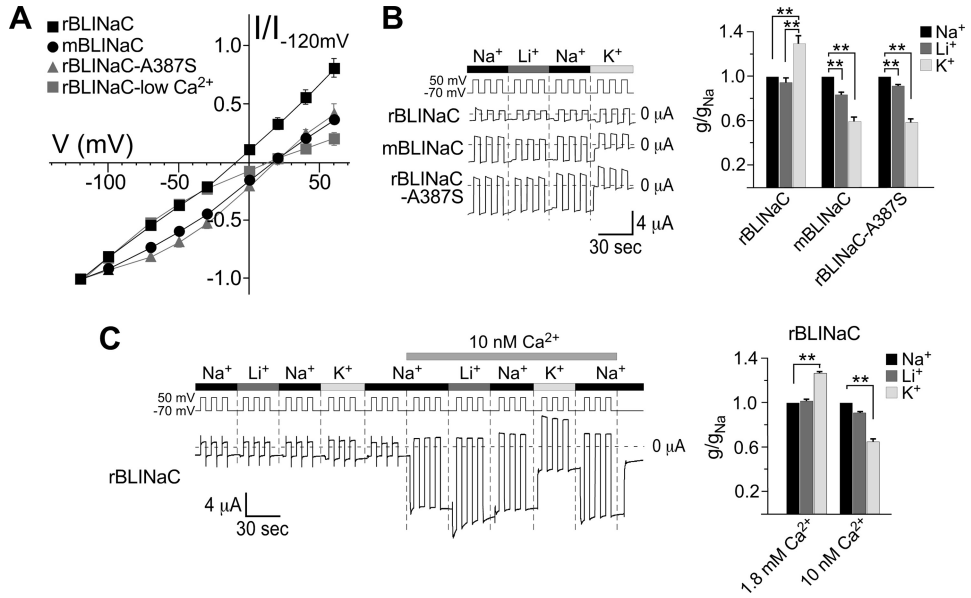

FIGURE 5. **Amino acid 387 determines ion selectivity of BLINaC.** *A*, normalized mean current-voltage relationships of amiloride-sensitive currents of rBLINaC (*black squares*), mBLINaC (*black circles*), and rBLINaC-A387S (*gray triangles*), determined in 1.8 mM $[Ca^{2+}]_e$. For rBLINaC, I-V relationships determined in 10 nM $[Ca^{2+}]_e$ are also shown (*gray squares*). The holding potential was increased stepwise from −120 to +60 mV (20- or 30-mV steps) in the absence and the presence of amiloride (100 μM for mBLINaC and rBLINaC-A387S, 4 mM for rBLINaC). Currents in the presence of amiloride were subtracted from currents in the absence of amiloride to yield the amiloride-sensitive currents at each holding potential. *B*, *left*, representative current traces for rBLINaC, mBLINaC, and rBLINaC-A387S. Currents were recorded at alternating holding potentials of −70 and +50 mV, in 1.8 mM $[Ca^{2+}]_e$ and 140 mM varying extracellular monovalent cations. *B*, *right*, conductances of mBLINaC, rBLINaC, and rBLINaC-A387S. Conductance was calculated according to the following equation: $g = ([I_{-70\ mV}]+[I_{+50\ mV}])/120$ mV. Conductances in the presence of Li^+ and K^+ were normalized to the conductance in the presence of Na^+. rBLINaC, $n = 8$; mBLINaC, $n = 8$; rBLINaC-A387S, $n = 11$; **, $p < 0.005$. *C*, *left*, representative current trace for rBLINaC in 1.8 mM and 10 nM $[Ca^{2+}]_e$. Holding potential was alternated between −70 and +50 mV. *C*, *right*, normalized conductances in 1.8 mM and 10 nM $[Ca^{2+}]_e$; $n = 9$; **, $p < 0.005$.

We then determined reversal potentials in low $[Ca^{2+}]_e$ (0.1 mM). The reversal potential of rBLINaC was significantly more positive (9.7 ± 0.8 mV, $n = 9$; Fig. 5*A*) than in physiological $[Ca^{2+}]_e$, indicating that Ca^{2+} block of rBLINaC is at least partly responsible for the different ion selectivities of rat and mouse BLINaC. In contrast, reversal potential of mBLINaC in low $[Ca^{2+}]_e$ (10 nM) was not significantly different (14.4 ± 1.8 mV, $n = 9$; data not shown) from reversal potential in physiological $[Ca^{2+}]_e$, as expected from the modest block by Ca^{2+}.

We further investigated ion selectivity by ion substitution experiments; whole oocyte currents were measured in physiological $[Ca^{2+}]_e$ with varying monovalent cations at a holding potential of −70 mV that was stepped to +50 mV for 5 s every 5 s. This protocol allowed simultaneous monitoring of current amplitude, membrane conductance, and degree of rectification. In these experiments, rBLINaC revealed a significantly larger conductance in the presence of K^+ than in the presence of Na^+ and Li^+ (Fig. 5*B*). In contrast, mBLINaC had a significantly larger conductance in the presence of Na^+ than in the presence of Li^+ and K^+ (Fig. 5*B*). These results agree with the more positive reversal potential and a higher Na^+ selectivity of mBLINaC (Fig. 5*A*). Similarly, for rBLINaC-A387S, ion substitution experiments revealed a significantly larger conductance in the presence of Na^+ than in the presence of Li^+ and K^+ (Fig. 5*B*).

No strong rectification was observed, except for currents through mBLINaC and rBLINaC-A387S in the presence of extracellular K^+, which were outwardly rectifying (Fig. 5*B*). Assuming higher intracellular Na^+ concentrations in oocytes expressing mBLINaC or rBLINaC-A387S, the outward currents of mBLINaC- and rBLINaC-A387S-expressing oocytes in the presence of extracellular K^+ were likely carried in part by Na^+, explaining the larger outward currents and the apparent outward rectification. In summary, in addition to differential apparent Ca^{2+} and amiloride affinities, rat and mouse BLINaC also have different ion selectivity. This difference is linked to Ca^{2+} block of rBLINaC and, as expected for such a link, the A387S substitution converted the ion selectivity of rBLINaC to that of mBLINaC.

For rBLINaC, we also substituted monovalent cations in the presence of low $[Ca^{2+}]_e$ (10 nM; Fig. 5*C*). A switch from high to low $[Ca^{2+}]_e$ generally increased BLINaC conductance (Fig. 5*C*), but more so in the presence of Na^+ and Li^+ than K^+, such that in low $[Ca^{2+}]_e$ the conductance in the presence of Na^+ was larger than in the presence of K^+, similar to mBLINaC (Fig. 5*B*). In contrast to mBLINaC, also in low $[Ca^{2+}]_e$ currents through rBLINaC did not rectify, which is expected if the rectification reflected higher intracellular Na^+ concentrations in oocytes expressing constitutively active mBLINaC. In summary, ion substitution experiments confirmed that mBLINaC is a Na^+-selective ion channel and that Na^+ selectivity of rBLINaC is higher in low $[Ca^{2+}]_e$ than in high $[Ca^{2+}]_e$.

BLINaC Is Permeable for H^+—The related channels ENaC and ASIC1a also conduct H^+, in addition to Na^+ (4, 24, 25). We therefore investigated H^+ permeability of BLINaC. Unlike ASICs, neither rat nor mouse BLINaC was activated by H^+. In contrast, stepwise reduction of the pH of the bath solution from 7.8 to 4.0 reduced current amplitude of mBLINaC (Fig. 6*A*), suggesting blockage of the inward (Na^+) current by H^+. Such a block does, however, not exclude permeation of H^+. Therefore, we completely replaced Na^+ by $NMDG^+$, which abolished inward currents at −70 mV, indicating that the large $NMDG^+$ cation does not permeate through mBLINaC. When we increased the H^+ concentration (pH 6.0, 5.0 and 4.0) in these Na^+-free solutions, we observed a weak inward current that was abolished when the pH was stepped back to 7.4 (Fig. 6*A*), suggesting that this current was carried by H^+ and that mBLINaC is permeable for H^+. The smaller currents of rBLINaC-expressing oocytes rendered characterization of H^+ permeability of rBLINaC more difficult, but, qualitatively, rBLINaC behaved similarly to mBLINaC.

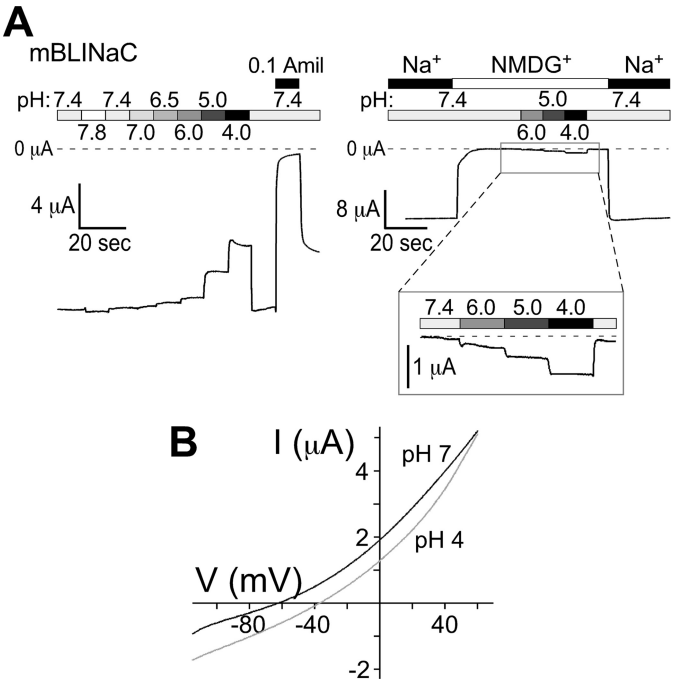

FIGURE 6. **BLINaC is proton-permeable.** *A*, representative current traces of an oocyte expressing mBLINaC. *Left*, bath solutions with varying proton concentrations were applied and exchanged every 10 s in the presence of Na^+. *Right*, after replacement of Na^+ by $NMDG^+$, increasing concentrations of protons were applied. The part of the current trace marked by the *box* is magnified at the *bottom*. *B*, representative current-voltage relationship of mouse BLINaC obtained in 1 mM Na^+ and with two different proton concentrations (100 nM corresponding to pH 7, *black curve*, and 100 μM corresponding to pH 4, *gray curve*). Voltage was ramped from −120 to +60 mV in 9 s.

We further investigated H^+ permeability of mBLINaC by strongly reducing the extracellular Na^+ concentration (1 mM) and looking for a dependence of the reversal potential on the H^+ concentration. Raising the H^+ concentration 1,000-fold from 100 nM to 100 μM (pH 7 to pH 4; Fig. 6*B*) significantly shifted the reversal potential by 19.4 mV ± 2.2 mV (from −64.6 ± −5.6 mV to −45.2 ± 8.2 mV, $n = 8$; $p \ll 0.001$). This corresponds to a relative permeability ratio P_H/P_{Na} of 7.4 ± 0.6 (see "Experimental Procedures"). Hence, mBLINaC is highly permeable for H^+, similar to ASIC1a (4, 25).

For rBLINaC, we investigated the dependence of the reversal potential on the H^+ concentration in 100 μM $[Ca^{2+}]_e$, a Ca^{2+} concentration at which the channel is partially activated (Fig. 1). Raising the H^+ concentration from 100 nM to 100 μM (pH 7 to pH 4), significantly shifted the reversal potential by 13.1 mV ± 2 mV (from −31.5 ± −2.3 mV to −18.4 ± 1.5 mV, $n = 10$; $p \ll 0.001$; results not shown). This corresponds to a relative permeability ratio P_H/P_{Na} of 4.5 ± 0.6. To test whether $[Ca^{2+}]_e$ affects the permeability for H^+ we repeated the experiment in the presence of a 100-fold lower Ca^{2+} concentration (1 μM), at which the channel is almost fully activated (Fig. 1). Under these conditions, the reversal potential shifted by 9 mV ± 0.3 mV (from −31.3 ± −0.6 mV to −22.3 ± 0.7 mV, $n = 10$; $p \ll 0.001$; results not shown), which is not significantly different from the shift in 100 μM $[Ca^{2+}]_e$ ($p = 0.8$) and which corresponds to a relative permeability ratio P_H/P_{Na} of 2.9 ± 0.3. Taken together, these results show that also rBLINaC is permeable for H^+ and that, in contrast to its relative Na^+ and K^+ permeabilities, its H^+ permeability is not significantly affected by $[Ca^{2+}]_e$.

DISCUSSION

Our study has two key findings: (i) rBLINaC is strongly inhibited by extracellular Ca^{2+} and (ii) mBLINaC is constitutively open, due to a much lower apparent Ca^{2+} affinity. In a previous study (11), rBLINaC was characterized by small current amplitudes but could be activated by introduction of a gain-of-function mutation. This mutation replaces an amino acid with a small side chain at the beginning of TMD2 (Ala^{443} in BLINaC) by an amino acid with a large side chain. Immediately after this so-called degenerin site (26), in BLINaC there is an Asp residue (Asp^{444}) that is conserved in most ASICs and that has been shown to be crucial for open channel Ca^{2+} block of ASIC1a (18). We now show that rBLINaC is strongly inhibited by physiological concentrations of extracellular Ca^{2+}. The gain-of-function mutation probably relieves Ca^{2+} inhibition. rBLINaC was half-maximally blocked by 10 μM extracellular Ca^{2+} (Fig. 1*B*). Because it is unlikely that such a low concentration will be reached physiologically, rBLINaC presumably requires an as yet unknown ligand for robust activation. Peptide-gated HyNaCs (6) are also inhibited by extacellular Ca^{2+},[3] showing that the gating of BLINaC shares fundamental features with the gating of ASICs and HyNaCs. Therefore, we speculate that rBLINaC is activated by an extracellular ligand, possibly a peptide.

Similar to rBLINaC, mBLINaC activity may be enhanced by an extracellular ligand, but clearly mBLINaC is constitutively open at physiological concentrations of extracellular Ca^{2+}. The large amplitudes of mBLINaC currents were comparable with amplitudes of ENaC currents in oocytes (23, 27), suggesting that, similar to ENaC, mBLINaC is physiologically a constitutively open channel. Furthermore, considering the rather high Na^+ selectivity of mBLINaC and the predominant expression of BLINaC in nonneuronal tissues (11), this finding suggests that BLINaC is an epithelial Na^+ channel. Further studies revealing the cellular expression pattern of the BLINaC protein in different tissues are needed to clarify this issue.

We identified a single amino acid substitution (Ala in rBLINaC, Ser in mBLINaC) that explains (i) the different apparent Ca^{2+} affinities, (ii) the different amiloride sensitivities, and (iii) the different ion selectivities of rBLINaC and mBLINaC. Given that the side chains of Ala and Ser residues differ only in one hydroxyl group, the profound effects of this amino acid substitution were surprising. A serine is invariably conserved at the corresponding position in all ASICs and HyNaCs, suggesting an important function for these ligand-gated channels. Because BLINaC and ASICs are closely related (6, 11), the crystal structure of chicken ASIC1 (cASIC1) (28) gives a first indication of the position of the critical residue in the ECD of BLINaC. The ECD of cASIC1 is composed of five subdomains, the palm, finger, thumb, knuckle, and β-ball domains, which assemble in a structure that resembles a clenched hand (28). Like mBLINaC, cASIC1 has a serine at the critical position (Ser^{376}), which local-

[3] S. Dürrnagel and S. Gründer, unpublished data.

izes to β-sheet 10 within the palm domain (28). Ser^{376} of cASIC1 is far (~50 Å) away from the ion pore, excluding a direct contribution to the pore. Moreover, because it is unlikely that A387 of rBLINaC directly binds Ca^{2+} or amiloride, it is highly likely that it affects apparent Ca^{2+} and amiloride affinities as well as ion selectivity by an allosteric mechanism.

Previously, it was found that rBLINaC is an unselective cation channel and that the DEG mutation increases Na^+ selectivity of the channel (11). Our results confirm that in the presence of physiological $[Ca^{2+}]_e$, rBLINaC does not select between monovalent cations. In addition, we found that in the presence of low $[Ca^{2+}]_e$ (0.1 mM) selectivity for Na^+ increases (Fig. 5). If Ca^{2+} inhibition were due to a simple open channel block, a change in ion selectivity of the pore would be rather surprising. Therefore, it is likely that removal of Ca^{2+} not only unblocks the ion pore but in addition induces a conformational change of the protein accompanied by open gating of the channel. A similar allosteric mechanism is also likely for Ca^{2+} inhibition of ASICs (18, 29) and HyNaCs.[3] In cASIC1, the side chain of Ser^{376} points toward β-sheet 8 in the palm domain of an adjacent subunit. We speculate that gating of BLINaC involves conformational changes at subunit-subunit interfaces, invoking β-sheets 10 and 8 with residue Ser^{376} occupying a critical position. In this model, the presence of a serine at position 376 in mBLINaC would strongly stabilize the open state of the channel, opening the channel in the absence of a putative ligand, whereas an alanine at position 376 would stabilize the closed state of the channel, rendering rBLINaC inactive in the absence of this putative ligand.

In summary, we propose that there are at least two states of BLINaC: one state of low activity with Ca^{2+} tightly bound and an unselective ion pore and one state of high activity with no Ca^{2+} bound and a Na^+ selective ion pore. At rest, rBLINaC would be predominantly in the first, low activity state whereas mBLINaC would be predominantly in the second, high activity state. A putative extracellular ligand would shift the equilibrium distribution between these two states for rBLINaC (and perhaps mBLINaC).

At present, it is a complete puzzle why rBLINaC is closed at rest whereas mBLINaC is constitutively open. Perhaps these differences correlate with species differences in the abundance of the putative ligand and/or with species differences in the required regulation of the ion transport pathway that is mediated by BLINaC.

Acknowledgment—We thank A. Oslender-Bujotzek for expert technical assistance.

REFERENCES

1. Kellenberger, S., and Schild, L. (2002) *Physiol. Rev.* **82,** 735–767
2. Canessa, C. M., Horisberger, J. D., and Rossier, B. C. (1993) *Nature* **361,** 467–470
3. O'Hagan, R., Chalfie, M., and Goodman, M. B. (2005) *Nat. Neurosci.* **8,** 43–50
4. Waldmann, R., Champigny, G., Bassilana, F., Heurteaux, C., and Lazdunski, M. (1997) *Nature* **386,** 173–177
5. Lingueglia, E., Champigny, G., Lazdunski, M., and Barbry, P. (1995) *Nature* **378,** 730–733
6. Golubovic, A., Kuhn, A., Williamson, M., Kalbacher, H., Holstein, T. W., Grimmelikhuijzen, C. J., and Gründer, S. (2007) *J. Biol. Chem.* **282,** 35098–35103
7. Dürrnagel, S., Kuhn, A., Tsiairis, C. D., Williamson, M., Kalbacher, H., Grimmelikhuijzen, C. J., Holstein, T. W., and Gründer, S. (2010) *J. Biol. Chem.* **285,** 11958–11965
8. Babini, E., Geisler, H. S., Siba, M., and Gründer, S. (2003) *J. Biol. Chem.* **278,** 28418–28426
9. Canessa, C. M., Schild, L., Buell, G., Thorens, B., Gautschi, I., Horisberger, J. D., and Rossier, B. C. (1994) *Nature* **367,** 463–467
10. Waldmann, R., Champigny, G., Bassilana, F., Voilley, N., and Lazdunski, M. (1995) *J. Biol. Chem.* **270,** 27411–27414
11. Sakai, H., Lingueglia, E., Champigny, G., Mattei, M. G., and Lazdunski, M. (1999) *J. Physiol.* **519,** 323–333
12. Gründer, S. (2000) in *Channelopathies* (Lehmann-Horn, F., and Jurkat-Rott, K., eds) pp. 277–297, Elsevier, Amsterdam
13. Sluka, K. A., Winter, O. C., and Wemmie, J. A. (2009) *Curr. Opin. Drug Discov. Devel.* **12,** 693–704
14. Schaefer, L., Sakai, H., Mattei, M., Lazdunski, M., and Lingueglia, E. (2000) *FEBS Lett.* **471,** 205–210
15. Gründer, S., and Chen, X. (2010) *Int. J. Physiol. Pathophysiol. Pharmacol.* **2,** 73–94
16. Babini, E., Paukert, M., Geisler, H. S., and Gründer, S. (2002) *J. Biol. Chem.* **277,** 41597–41603
17. Immke, D. C., and McCleskey, E. W. (2003) *Neuron* **37,** 75–84
18. Paukert, M., Sidi, S., Russell, C., Siba, M., Wilson, S. W., Nicolson, T., and Gründer, S. (2004) *J. Biol. Chem.* **279,** 18783–18791
19. Bässler, E. L., Ngo-Anh, T. J., Geisler, H. S., Ruppersberg, J. P., and Gründer, S. (2001) *J. Biol. Chem.* **276,** 33782–33787
20. Madeja, M., Musshoff, U., and Speckmann, E. J. (1995) *J. Neurosci. Methods* **63,** 211–213
21. Chen, X., Paukert, M., Kadurin, I., Pusch, M., and Gründer, S. (2006) *Neuropharmacology* **50,** 964–974
22. Nilius, B., Prenen, J., Droogmans, G., Voets, T., Vennekens, R., Freichel, M., Wissenbach, U., and Flockerzi, V. (2003) *J. Biol. Chem.* **278,** 30813–30820
23. Schild, L., Schneeberger, E., Gautschi, I., and Firsov, D. (1997) *J. Gen. Physiol.* **109,** 15–26
24. Gilbertson, T. A., Roper, S. D., and Kinnamon, S. C. (1993) *Neuron* **10,** 931–942
25. Chen, X., and Gründer, S. (2007) *J. Physiol.* **579,** 657–670
26. Driscoll, M., and Chalfie, M. (1991) *Nature* **349,** 588–593
27. Gründer, S., Jaeger, N. F., Gautschi, I., Schild, L., and Rossier, B. C. (1999) *Pflügers Arch.* **438,** 709–715
28. Jasti, J., Furukawa, H., Gonzales, E. B., and Gouaux, E. (2007) *Nature* **449,** 316–323
29. Zhang, P., Sigworth, F. J., and Canessa, C. M. (2006) *J. Gen. Physiol.* **127,** 109–117